This manuscript has been submitted for publication to Geochemical Perspectives Letters on 19 March 2024. Please note that, despite having undergoneone one round of peer-review, the manuscript has not yet been accepted for publication (corrections recently returned to journal). Subsequent versions of this manuscript may have slightly different content. Feel free to reach out the corresponding author. We welcome constructive feedback.

Medieval and recent SO_2 budgets in the Reykjanes Peninsula: implication for future hazard

A. Caracciolo[1], E. Bali[1], E. Ranta[2], S. A. Halldórsson[1] , G. H. Guðfinnsson[1],B.V. Óskarsson[3]

(1) NordVulk, Institute of Earth Sciences, University of Iceland, 102, Reykjavík, Iceland.

(2) Department of Geosciences and Geography, University of Helsinki, Finland

(3) Icelandic Institute of Natural History, Urriðaholsstræti 6–8, Garðabær,7110, Iceland

Corresponding author: Alberto Caracciolo (alberto@hi.is)

Abstract

Exposure to volcanic SO_2 can have adverse effects on human health, with severe respiratory disorders documented on short- and long-term timescales. Here, we use melt inclusion and groundmass glass data to calculate potential syn-eruptive SO_2 emissions during the medieval and the recent 2021-2024 eruptions across the Reykjanes peninsula, the most populated area of Iceland that has recently undergone magmatic reactivation with the 2021-2024 eruptions at Fagradalsfjall and Svartsengi. We target 16 individual eruptions from the medieval volcanic cycle at the RP, the 800-1240 AD Fires, along with the 2021-23 Fagradalsfjall eruptions and the 2023-24 eruptions at Sundhnúksgígar. We calculate potential SO_2 emissions across the RP to be in the range 0.004-6.3 Mt. These estimates correspond to mean daily SO_2 emissions in the range 1000-111000 tons/day, higher than the mean SO_2 measurements of 5240 ± 2700 tons/day during the 2021 Fagradalsfjall eruption. By using pre-eruptive sulfur values preserved in undegassed melt inclusions, we develop an empirical approach to calculate best- and worst-case potential SO_2 emission scenarios of any past or ongoing RP eruption of known effusion rate. We conclude that the potential sulfur emissions across the RP can be significantly higher than observed during the 2021 Fagradalsfjall eruption, mainly because of the more evolved nature and higher sulfur contents of magmas erupted during the medieval time. Based on dominant NW wind directions on the RP, eruptions in Brennisteinsfjöll pose the greatest health hazard to the capital area. Sulfate aerosol produced during long-term eruptions may impact visibility and air quality in the Keflavík airport area. Our findings enable assessment of SO_2 emission scenarios of future eruptions across the RP and can be used together with gas dispersal models to forecast SO_2 pollution at ground level and its impact on human health.

Introduction

The release of volcanic gases and aerosols during volcanic eruptions can significantly impact the air quality and climate (e.g. Ilyinskaya *et al.*, 2017), as well as the biodiversity (e.g., Weiser *et al.*, 2022). Among volcanic gases, sulfur species (SO_2, H_2S) and associated aerosols (SO_4, H_2SO_4) are the most critical airborne hazard to human health, with short and long-term impacts that have been recorded at variable distances from eruptive vents (e.g., Horwell et al. 2023, Stewart et al. 2022; Ilyinskaya et al., 2017; Schmidt et al., 2015). For example, several studies have associated cardiorespiratory issues with volcanic sulfur emissions (e.g., Carlsen *et al.*, 2021; Heaviside *et al.*, 2021). Hence, a detailed knowledge of potential sulfur releases of active volcanoes located in densely populated areas is critical to understand air quality hazards of future volcanic eruptions. This is the case of the Reykjanes Peninsula (RP) in southwest Iceland, an active spreading area segmented into five volcanic systems, which from west to east are Reykjanes, Svartsengi, Fagradalsfjall, Krýsuvík and Brennisteinsfjöll. The latest magmatic period in the RP occurred ~800 years ago (Sæmundsson et al., 2020) but knowledge about sulfur outputs during those eruptions has been lacking thus far. Each volcanic system on the RP tends to activate during individual magmatic periods (Sæmundsson et al., 2020) and the recent 2021-2024 Fagradalsfjall and Svartsengi eruptions (Barsotti et al., 2023; Sigmundsson et al. 2024) suggest the potential initiation of a new eruptive period in an area that hosts ~70% of the Icelandic population. Consequently, there is an increased societal need for a deeper understanding of sulfur emissions across the RP, which is crucial for a comprehensive assessment of sulfur's impact during future eruptions and its potential consequences for human health.

Here, we focus on magmatic units erupted in the volcanic systems of Reykjanes, Svartsengi, Krýsuvík and Brennisteinsfjöll in the RP during the last medieval eruptive cycle, which occurred between the 8th century and 1240 AD, hereafter referred to as the 800-1240 AD Fires (Caracciolo et al., 2023; Peate et al., 2009). Additionally, we target the 2021-23 Fagradalsfjall eruptions and the December 2023, January 2024 and February 2024 eruptions at Sundhnúksgígar in Svartsengi. We calculate syn-eruptive sulfur release and potential sulfur emissions of 19 geologically and petrochemically well characterized

magmatic units (Caracciolo et al., 2023; Peate et al., 2009) and compare those with sulfur emissions from the 2021 Fagradalsfjall eruption (Barsotti et al., 2023; Halldórsson et al., 2022). Also, we estimate daily SO_2 emissions and develop an empirical approach to calculate worst- and best-case potential sulfur emissions for any eruption of a given volume emplaced in the RP.

Samples and methods

Scoria samples were collected from multiple vents within individual eruptive units of the 800-1240 AD Fires (Caracciolo et al., 2023). Here, we present new sulfur (S) data for the same groundmass glass (n=889) and melt inclusions (MIs) (n=416) dataset published in Caracciolo et al. (2023). Additionally, we include new MI and groundmass glass data from the 2022 and 2023 Fagradalsfjall eruptions, as well as data from the eruptions at Sundhnúksgígar that occurred in the Svartsengi volcanic system in December 2023, January 2024 and February 2024. S was analysed by electron microprobe analyser (EMPA) at the University of Iceland using the same analytical settings as in Caracciolo *et al.* (2020) and MI compositions have been corrected for post-entrapment processes (PEP) (Caracciolo et al. 2023).

Here, we use of the 'petrological method' (Devine et al., 1984) to calculate eruptive sulfur emissions based on the difference between S concentrations in mineral-hosted MIs and S concentrations measured in groundmass glass (ΔC_S). The idea behind this reconstruction method is that melt inclusions with similar composition to erupted melts preserve the pre-eruptive volatile content, and quenched groundmass glasses provide an estimate of the post-eruptive volatile content. For the different magmatic units, the highest S concentration measured in PEP-corrected MIs ($C_{S\,MI}$) is selected as the pre-eruptive S concentration, whereas the lowest S concentration in groundmass glasses ($C_{S\,glass}$) is chosen as the post-eruptive S concentration. By combining the mass of erupted magmas with the mass of S released, we can assess vent syn-eruptive SO_2 emissions (M_s) of individual eruptions (eq. 1 and eq. 2 in the supplement) (e.g., Bali *et al.*, 2018; Thordarson *et al.*, 2003). Furthermore, we calculate the magnitude of potential SO_2 emissions (potential M_s), which refers to complete degassing of all pre-eruptive sulfur ($C_{S\,glass} = 0$) and reflects the maximum amount of SO_2

that a specific eruption could potentially have released, assuming that there is no degassing of unerupted magma. This reconstruction method has been showed to have matched field-based volatile measurements exceptionally well during the 2014-15 Holuhraun eruption (Bali et al., 2018; Pfeffer et al., 2018) and the 2021 Fagradalsfjall eruption (this work, Table 1).

Sulfur concentrations in MI and groundmass glass

Sulfur concentration in MIs is in the range 200-1900 ppm, with a relatively large variability of S at a given MI Mg#. Particularly, the most primitive MIs (Mg#>65), exclusively preserved in Reykjanes and Krýsuvík, record S contents in the range 580-1070 ppm (Fig. 1). S concentration in PEP-corrected MI compositions increases with decreasing MI Mg#, as expected for melt compositions controlled by fractional crystallization. MIs from the 2023-24 eruptions at Sundhnúksgígar record pre-eruptive S concentrations in the range 1400-1600 ppm, in agreement with MI data from the medieval eruptions (Fig. 1b). MIs from the 2022-23 Fagradalsfjall eruptions closely match S concentrations measured in the 2021 products (Fig. 1c). Groundmass glasses from Brennisteinsfjöll have mean S contents in the range 150-280 ppm, lower than mean S contents measured in glasses from the other volcanic systems (280-450 ppm) (Fig. 1, Table 1). For comparison, MIs from the 2021 Fagradalsfjall eruption contain maximum S concentrations of 1200 ppm, whereas the groundmass glasses contain 20-200 ppm S. Sulfide globules were not observed in the erupted samples.

Assessing sulfur variability and degassing during the 800-1240 AD Fires

Considering that medieval and recent eruptions on the RP are likely sourced from mantle-derived melts of diverse compositions (Caracciolo et al., 2023; Harðardóttir et al., 2022; Halldórsson et al., 2022; Peate et al., 2009), including melts with variable S contents (Ranta *et al.*, 2022), we use our MI record to estimate S contents of the local enriched and depleted end-member melt components. We

distinguish between these components from the K_2O/TiO_2 variability, a robust tracer of mantle heterogeneities in Iceland (Halldórsson et al., 2022; Harðardóttir et al., 2022) (see supplement). Our modelling, considering that S behaves as an incompatible element in basaltic magmas, shows that most of the MI S variability can be explained by fractional crystallization (FC) and mixing of at least two end-member melt compositions (Fig. 1a-d).

In order to evaluate S saturation during magma ascent and fractional crystallization through the crust, we calculate sulfur content at sulfide saturation (SCSS) along a FC path, which reflects the amount of S^{2-} present in a melt in equilibrium with a sulfide phase (Smythe et al., 2017) (see supplement). Our modelling suggests that melts are sulfide undersaturated during most of magmatic fractionation across the RP (Fig. 1 and Fig. S3-S4). Only magmas from Svartsengi and Brennisteinsfjöll have a high likelihood to be sulfide saturated prior to eruptions. Furthermore, sulfide saturation is reached earlier during magmatic differentiation of enriched mantle-derived melts than depleted melts (Fig. 1).

Modelling of S degassing with Sulfur_X (Ding et al. 2023) suggests that basaltic melts erupted during the 800-1240 AD Reykjanes Fires are unlikely to degas significant amounts of S at known pre-eruptive magma storage depths (Caracciolo et al. 2023) and that significant S degassing only takes place during magma ascent in the last 0.2 kbar (<700 m) (Fig. S1).

Sulfur emissions across the RP

Sulfur release ranges between 1000-1770 ppm across the RP, a typical range for Icelandic rift basalts (Ranta et al. 2024), with the largest ΔC_s found in lavas from Svartsengi and Brennisteinsfjöll (Table 1). ΔC_s values can be scaled by the mass of erupted material to estimate M_s of individual eruptions, using published volumes of individual eruptive units, in the range 0.01 km^3 to 0.72 km^3 (Table 1). Using a melt density of 2700 kg/m^3 and assuming a bulk vesicularity of 15 vol%, we calculate M_s between 0.003-5.9 Mt (Fig. 2a). The most voluminous lavas found in Svartsengi and Brennisteinsfjöll released the highest mass of SO_2 into the atmosphere during the medieval time. The syn-eruptive SO_2 released by these latter voluminous lavas is approximately 2 to 6 times larger than syn-eruptive SO_2 emissions

during the 2021 Fagradalsfjall eruption, for which we estimated M_s = 0.78 Mt ($M_{s\ measured}$ =0.97±0.5, Barsotti et al. 2023). These are roughly between 20 to 70 % of the syn-eruptive SO_2 emissions estimated for the 2014-15 Holuhraun eruption (M_s = 10.5 Mt, Bali et al. 2018). We calculate SO_2 release of 0.06-0.07 Mt for the 2022 and 2023 Fagradalsfjall eruptions, respectively. However, for a given mass of melt, the 2021-23 Fagradalsfjall eruptions released a comparable mass of SO_2 (Table 1). Oppositely, the 2023-24 eruptions at Sundhnúksgígar slightly exceeded SO_2 emissions during the 2021-23 Fagradalsfjall eruptions (Table 1). Similarly, we have calculated potential M_s, the maximum mass of SO_2 that could potentially have been released during each eruption. Potential M_s across the RP ranges between 0.003-6.3 Mt and is only slightly higher than vent M_s, as most of the S is released into the atmosphere during eruptions rather than staying dissolved in the lava (Table 1).

Evaluating end-member scenarios of SO_2 emissions and hazard potential for future eruptions across the RP.

Based on the MI record of the 2021-23 Fagradalsfjall eruption (Halldórsson et al., 2022 and this work), the 2023-24 eruptions at Sundhnúksgígar and the 800-1240 AD Fires (this work), we constrain potential maximum (1900 ppm) and minimum (1170 ppm) pre-eruptive S concentrations and use these to estimate potential M_s of future eruptions in the RP. With these constraints, we developed an empirical approach to assess potential M_s for a given eruption of known lava volume, with important applications for forecasting the worst- and best-case scenarios of potential M_s of future eruptive events (Fig. 2b). For example, based on our approach, an eruption with an eruptive volume of 0.4 km^3, could release between 2.9 Mt and 4.1 Mt of SO_2. This method also has an application when it comes evaluating the long-term SO_2 impact of ongoing eruptions in the RP. If the mean magma effusion rate is known and fixed, one can roughly estimate the volume of the lava flow and calculate potential M_s at any given moment from the onset of the eruption. This provides a valuable tool to assess best- and worst-case scenarios for SO_2 pollution during ongoing events.

Eruptive M_s calculations are strongly dependent on lava flow volumes. Hence, when it comes to comparing the 800-1240 AD Fires with the 2021-24 eruptions, a more relevant parameter is the mean daily SO_2 emissions, which also is an important parameter from a hazard perspective. We have estimated daily SO_2 emissions for the 800-1240 AD Fires using mean output rates (MOR) calculated by Oskarsson et al. (2024), in the range 3-119 m^3/s (Table 1, Eq. 3 supplement). Mean daily SO_2 emissions during the medieval eruptions likely ranged between 1000 ton/day to 111000 ton/day (Fig. 2c). In comparison, during the 2021, 2022 and 2023 Fagradalsfjall eruptions, we calculate average daily SO_2 emissions of 5000, 3780 and 3360 ton/day, respectively. The estimate for the 2021 Fagradalsfjall eruption is in agreement with the majority of measured daily SO_2 emissions throughout the 2021 Fagradalsfjall eruption, in the range 1000-7600 ton/day (Esse et al., 2023), and with daily SO_2 emissions of 5240 ± 2700 ton/day, calculated assuming 0.97±0.5 Mt of total mass of SO_2 (Barsotti et al. 2023). Oppositely, the Dec. 2023 Sundhnúkar eruption released 32000 ton/day SO_2 (Table 1). Our calculations highlight that future eruptions in the RP may have the potential to release significantly more SO_2 on a daily basis than the 2021-24 eruptions.

SO_2 emissions during the 800-1240 AD Fires and the 2021-24 eruptions are small compared to those during the 2014-15 Holuhraun basaltic eruption (9.2 Mt SO_2, Pfeffer *et al.*, 2018). However, volcanic eruptions in the RP are potentially considered to be more hazardous due to their proximity to inhabited areas, to the international airport and to the large number of visitors expected at eruption sites (Fig. 3) (Barsotti et al. 2023). To assess the health hazard for potential future eruptions, we built seasonal wind roses, for the period 2012-2022, reflecting dominant wind speeds and directions in the RP (Hersbach et al. 2023). We find that most of the time prevailing winds blow towards the NW-NE, suggesting different SO_2 health hazards potential associated with eruptions within different volcanic systems (Fig. 3). The prevalent NW wind blowing direction suggests that volcanic SO_2 emissions could still be disruptive to the Keflavik airport area if there were a long-duration eruption. Even if eruptions in the RP produce little ash, sulfate aerosol in the atmosphere could reduce visibility and air quality (Pattantyus et al. 2018). Eruptions in Brennisteinsfjöll are the most hazardous for Reykjavík, especially

in spring and autumn seasons, as SO_2 is likely to be blown towards the capital area. Eruptions in Reykjanes pose minimal hazard as winds tend to blow away from inhabited areas. During assessment of possible eruptive scenarios in the RP, our estimates provide key input parameters to model the release and dispersion of volcanic SO_2 into the atmosphere. Our results can be used to inform SO_2 pollution hazard assessments for potential eruptive scenarios and prompt action and mitigation plans during ongoing volcanic crises in the RP.

Acknowledgement

This research was financially support by a NordVulk fellowship awarded to AC and by the Icelandic Research Fund (grant 228933-052). We acknowledge support from the Gosvá project, a research programme on the assessment of volcanic hazard risks in Iceland led by the Icelandic Meteorological Office (IMO). SAH acknowledges support from the Icelandic Research Fund (Grant #196139-051). We thank Christoph Kern, two anonymous reviewers, and editor Ambre Luguet for their constructive comments, which significantly improved the quality of the manuscript.

Figure Captions

Table 1. Eruptive units studied in this work and summary of main results. $C_{S\ MI}$= pre-eruptive S concentration. $C_{S\ glass}$ = post-eruptive S concentration. ΔC_S = sulfur emissions at the vent per unit mass of melt, accounting for crystallinity. $V_=$ bulk lava volume. V_{DRE} = Vesicle-free lava volume. M_s = Syn-eruptive SO_2 emissions at the vent. Potential M_s = potential SO_2 emissions. Lava volumes for the medieval eruptions are from Einarsson et al. (1991), Jónsson (1978) and Sigurgeirsson (2004). [a] Lava volume estimated by assuming a thickness of 5 m, consistent with average thicknesses of lava flows of known volumes with a similar aerial extent. [b] MOR values (within brackets) and uncertainty ranges for the medieval eruptions are from Óskarsson et al. (2024). [c] V and MOR from Pedersen et al. (2022). [d] V and MOR from Pedersen et al. (2024). *Lava volumes for the 2024 eruptions at Sundhnúksgígar are not available at the current stage.

Fig. 1. (a-d) Variation of S contents in groundmass glasses (filled circles) and PEP-corrected MIs (filled triangles) as a function of Mg# [Mg# = 100·Mg/(Mg+Fe^{2+}), Fe^{2+}/Fe^{tot} = 0.9] in samples from the 800-1240 AD Fires, the 2021-2023 Fagradalsfjall eruptions and the 2023-24 eruptions at Sundhnúksgígar. Data from the 2021 Fagradalsfjall eruption are from Halldórsson *et al.* (2022). Red and blue solid lines indicate fractional crystallization paths calculated for a geochemically enriched and depleted initial melt compositions, respectively (see supplement). The black dotted curve indicates SCSS along an empirical fractional crystallization path calculated after Smythe *et al.* (2017), implemented in PySulfSat (Wieser and Gleeson, 2022).

Fig. 2. (a) Variation of vent M_s (b) Magnitude of potential M_s as a function of eruption volume for the 800-1240 AD Fires, the 2021-23 Fagradalsfjall eruptions and the 2023 Sundhnúkar eruption. At a given volume, straight lines allow to calculate potential M_s corresponding to maximum and minimum pre-eruptive S concentrations measured across the RP. Inset plot show most common potential M_s across the RP (c) Daily SO_2 emissions are calculated using MOR values and associated uncertainties from Óskarsson et al. (2024). Blue histogram indicates measured SO_2 emissions during the 2021 Fagradalsfjall eruption (Esse et al., 2023). Data are coloured according to the volcanic system and only lavas with known volumes or MORs are included in the plots.

Fig. 3. Simplified geological map of the RP and lava flows emplaced during the 800 – 1240 AD Fires. The map also illustrates the aerial extent of the 2021 (Pedersen et al., 2022), 2022 (Gunnarson et al., 2023) and 2023 (Belart et al. 2023) Fagradalsfjall lavas. Data from the 2023-24 eruptions at Sundhnúksgígar are from the Landmælingar Íslands geoserver (gis.lmi.is/geoserver). When possible, lava flows are coloured according to calculated syn-eruptive SO_2 emissions, ranging from 0.1 to 6 Mt. Orange outlines show urban areas. Numbers reflect the different lava units as listed in table 1. Seasonal wind roses reflect data at 900 mPa (~1000 m a.s.l), which was the most common SO_2 injection

altitude during the 2021 Fagradalsfjall eruption (Esse et al. 2023). Spokes indicate the direction the wind is blowing from, and the length of each spoke shows the frequency. Wind data were extracted from ERA5 (Hersbach et al. 2023).

References

Bali, E., Hartley, M.E., Halldórsson, S.A., Gudfinnsson, G.H., Jakobsson, S., 2018. Melt inclusion constraints on volatile systematics and degassing history of the 2014–2015 Holuhraun eruption, Iceland. Contributions to Mineralogy and Petrology 173, 9. https://doi.org/10.1007/s00410-017-1435-0

Barsotti, S., Parks, M.M., Pfeffer, M.A., Óladóttir, B.A., Barnie, T., Titos, M.M., Jónsdóttir, K., Pedersen, G.B.M., Hjartardóttir, R., Stefansdóttir, G., Johannsson, T., Arason, Gudmundsson, M.T., Oddsson, B., Þrastarson, R.H., Ófeigsson, B.G., Vogfjörd, K., Geirsson, H., Hjörvar, T., von Löwis, S., Petersen, G.N., Sigurðsson, E.M., 2023. The eruption in Fagradalsfjall (2021, Iceland): how the operational monitoring and the volcanic hazard assessment contributed to its safe access. Natural Hazards. https://doi.org/10.1007/s11069-022-05798-7

Belart, J.M.C., Pinel, V., Reynolds, H.I., Berthier, E., Gunnarson, S.R., 2023. Digital Elevation Models (DEMs) and lava outlines from the 2023 Litla-Hrútur eruption, Iceland, from Pléiades satellite stereoimages. https://doi.org/10.5281/zenodo.10133203

Caracciolo, A., Bali, E., Guðfinnsson, G.H., Kahl, M., Halldórsson, S.A., Hartley, M.E., Gunnarsson, H., 2020. Temporal evolution of magma and crystal mush storage conditions in the Bárðarbunga-Veiðivötn volcanic system, Iceland. Lithos 352–353. https://doi.org/10.1016/j.lithos.2019.105234

Caracciolo, A., Bali, E., Halldórsson, S.A., Gudfinnsson, G.H., Kahl, M., Þórðardóttir, I., Pálmadóttir, G.L., Silvestri, V., 2023. Magma plumbing systems and timescale of magmatic processes during historical magmatism on Reykjanes Peninsula. Earth and Planetary Science Letters 621, 118378.

https://doi.org/10.1016/j.epsl.2023.118378

Carlsen, H.K., Valdimarsdóttir, U., Briem, H., Dominici, F., Finnbjornsdottir, R.G., Jóhannsson, T., Aspelund, T., Gislason, T., Gudnason, T., 2021. Severe volcanic SO2 exposure and respiratory morbidity in the Icelandic population – a register study. Environmental Health: A Global Access Science Source 20, 1–12. https://doi.org/10.1186/s12940-021-00698-y

Devine, D., Sigurdsson, H., Davis, A.N., 1984. Estimates of sulfur and chlorine yield to the atmosphere from volcanic eruptions and potential climatic effects. Journal of Geophysical Research 89, 6309–6325.

Ding, S., Plank, T., Wallace, P.J., Rasmussen, D.J., 2023. Sulfur_X: A Model of Sulfur Degassing During Magma Ascent. Geochemistry, Geophysics, Geosystems 24. https://doi.org/10.1029/2022GC010552

Einarsson, S., Johannesson, H., Sveinbjörnsdóttir, A.E., 1991. Krísuvíkureldar II. Kapelluhraun og gátan um aldur Hellnahrauns. Jokull 41.

Esse, B., Burton, M., Hayer, C., Pfeffer, M.A., Barsotti, S., Theys, N., Barnie, T., Titos, M., 2023. Satellite derived SO2 emissions from the relatively low-intensity, effusive 2021 eruption of Fagradalsfjall, Iceland. Earth and Planetary Science Letters 619, 118325. https://doi.org/10.1016/j.epsl.2023.118325

Fortin, M.A., Riddle, J., Desjardins-Langlais, Y., Baker, D.R., 2015. The effect of water on the sulfur concentration at sulfide saturation (SCSS) in natural melts. Geochimica et Cosmochimica Acta 160, 100–116. https://doi.org/10.1016/j.gca.2015.03.022

Gunnarson, S.R., Belart, J.M.C., Óskarsson, B. V., Gudmundsson, M.T., Högnadóttir, T., Pedersen, G.B.M., Dürig, T., Pinel, V., 2023. Automated processing of aerial imagery for geohazards monitoring: Results from Fagradalsfjall eruption, SW Iceland, August 2022 [WWW Document]. Zenodo. https://doi.org/10.5281/ZENODO.7871187

Halldórsson, S.A., Marshall, E.W., Caracciolo, A., Matthews, S., Bali, E., Rasmussen, M.B., Ranta, E., Robin, J.G., Gudfinnsson, G.H., Sigmarsson, O., Maclennan, J., Jackson, M.G., Whitehouse, M.J.,

Jeon, H., van der Meer, Q.H.A., Mibei, G.K., Kalliokoski, M.H., Repczynska, M.M., Rúnarsdóttir, R.H., Sigurðsson, G., Pfeffer, M.A., Scott, S.W., Kjartansdóttir, R., Barbara, K., Kleine, B.I., Oppenheimer, C., Aiuppa, A., Ilyinskaya, E., Bitetto, M., Giudice, G., Stefánsson, A., 2022. Rapid shifting of a deep magmatic source at Fagradalsfjall volcano, Iceland. Nature 609. https://doi.org/10.1038/s41586-022-04981-x

Harðardóttir, S., Matthews, S., Halldórsson, S.A., Jackson, M.G., 2022. Spatial distribution and geochemical characterization of Icelandic mantle end-members: Implications for plume geometry and melting processes. Chemical Geology 604. https://doi.org/10.1016/j.chemgeo.2022.120930

Heaviside, C., Witham, C., Vardoulakis, S., 2021. Potential health impacts from sulphur dioxide and sulphate exposure in the UK resulting from an Icelandic effusive volcanic eruption. Science of the Total Environment 774, 145549. https://doi.org/10.1016/j.scitotenv.2021.145549

Hersbach, H., Bell, B., Berrisford, P., Biavati, G., Horányi, A., Muñoz Sabater, J., Nicolas, J., Peubey, C., Radu, R., Rozum, I., Schepers, D., Simmons, A., Soci, C., Dee, D., Thépaut, J-N. (2023): ERA5 hourly data on pressure levels from 1940 to present. Copernicus Climate Change Service (C3S) Climate Data Store (CDS), DOI: 10.24381/cds.bd0915c6 (Accessed on 26-10-2023)

Horwell, C.J., Baxter, P.J., Damby, D.E., Elias, T., Ilyinskaya, E., Sparks, R.S.J., Stewart, C. and Tomasek, I., 2023. The International Volcanic Health Hazard Network (IVHHN): Reflections on twenty years of progress. *Frontiers in Earth Science*, *11*, p.1213363.

Ilyinskaya, E., Schmidt, A., Mather, T.A., Pope, F.D., Witham, C., Baxter, P., Jóhannsson, T., Pfeffer, M., Barsotti, S., Singh, A., Sanderson, P., Bergsson, B., McCormick Kilbride, B., Donovan, A., Peters, N., Oppenheimer, C., Edmonds, M., 2017. Understanding the environmental impacts of large fissure eruptions: Aerosol and gas emissions from the 2014–2015 Holuhraun eruption (Iceland). Earth and Planetary Science Letters 472, 309–322. https://doi.org/10.1016/j.epsl.2017.05.025

Jónsson, J., 1978. Jarðfræðikort af Reykjanesskaga : 1. Skýringar við jarðfræðikort 2. Jarðfræðikort.

Orkustofnun.

Óskarsson, B. V. , Askew, R. A., Guðmundsson, H. (2024) Assessing the mean output rate (MOR) of past effusive basaltic eruptions - a look at the postglacial volcanism of the Reykjanes Peninsula in Iceland. Preprint, submitted to Bullettin of Volcanology https://doi.org/10.31223/X5CH68

Pattantyus, A.K., Businger, S., Howell, S.G., 2018. Review of sulfur dioxide to sulfate aerosol chemistry at Kīlauea Volcano, Hawai'i. Atmospheric Environment 185, 262–271. https://doi.org/10.1016/j.atmosenv.2018.04.055

Peate, D.W., Baker, J.A., Jakobsson, S.P., Waight, T.E., Kent, A.J.R., Grassineau, N. V., Skovgaard, A.C., 2009. Historic magmatism on the Reykjanes Peninsula, Iceland: A snap-shot of melt generation at a ridge segment. Contributions to Mineralogy and Petrology 157, 359–382. https://doi.org/10.1007/s00410-008-0339-4

Pedersen, G.B.M., Belart, J.M.C., Óskarsson, B.V., Gudmundsson, M.T., Gies, N., Högnadóttir, T., Hjartardóttir, Á.R., Pinel, V., Berthier, E., Dürig, T., Reynolds, H.I., Hamilton, C.W., Valsson, G., Einarsson, P., Ben-Yehosua, D., Gunnarsson, A., Oddsson, B., 2022. Volume, Effusion Rate, and Lava Transport During the 2021 Fagradalsfjall Eruption: Results From Near Real-Time Photogrammetric Monitoring. Geophysical Research Letters 49, 1–11. https://doi.org/10.1029/2021GL097125

Pedersen, G. B. M., Belart, J. M. C., Óskarsson, B. V., Gunnarson, S. R., Gudmundsson, M. T., Reynolds, H. I., Valsson, G., Högnadóttir, T., Pinel, V., Parks, M. M., Drouin, V., Askew, R. A., Dürig, T., and Þrastarson, R. H, 2024: Volume, effusion rates and lava hazards of the 2021, 2022 and 2023 Reykjanes fires: Lessons learned from near real-time photogrammetric monitoring, EGU General Assembly 2024, Vienna, Austria, 14–19 Apr 2024, EGU24-10724, 2024. https://meetingorganizer.copernicus.org/EGU24/EGU24-10724.html

Pfeffer, M.A., Bergsson, B., Barsotti, S., Stefánsdóttir, G., Galle, B., Arellano, S., Conde, V., Donovan, A., Ilyinskaya, E., Burton, M., Aiuppa, A., Whitty, R.C.W., Simmons, I.C., Arason, Þ., Jónasdóttir,

E.B., Keller, N.S., Yeo, R.F., Arngrímsson, H., Jóhannsson, Þ., Butwin, M.K., Askew, R.A., Dumont, S., Von Löwis, S., Ingvarsson, Þ., La Spina, A., Thomas, H., Prata, F., Grassa, F., Giudice, G., Stefánsson, A., Marzano, F., Montopoli, M., Mereu, L., 2018. Ground-Based measurements of the 2014-2015 holuhraun volcanic cloud (Iceland). Geosciences (Switzerland) 8, 1–25. https://doi.org/10.3390/geosciences8010029

Ranta, E., Halldórsson, S.A., Óladóttir, B.A., Pfeffer, M.A., Caracciolo, A., Bali, E., Guðfinnsson, G.H., Kahl, M. and Barsotti, S., 2024. Magmatic Controls on Volcanic Sulfur Emissions at the Iceland Hotspot. Pre-print. https://doi.org/10.31223/X51102

Sæmundsson, K., Sigurgeirsson, M., Friðleifsson, G.Ó., 2020. Geology and structure of the Reykjanes volcanic system, Iceland. Journal of Volcanology and Geothermal Research 391, 106501. https://doi.org/10.1016/j.jvolgeores.2018.11.022

Sigmundsson, F., Parks, M., Geirsson, H., Hooper, A., Drouin, V., Vogfjörd, K.S., Ófeigsson, G., Greiner, S.H.M., Yang, Y., Lanzi, C., Pascale, G.P. De, Jónsdóttir, K., Hreinsdóttir, S., Tolpekin, V., Friðriksdóttir, H.M., Einarsson, P., Barsotti, S., 2024. Fracturing and tectonic stress drives ultrarapid magma flow into dikes 2838, 1–12. https://doi.org/10.1126/science.adn2838

Schmidt, A., Leadbetter, S., Theys, N., Carboni, E., Witham, C.S., Stevenson, J.A., Birch, C.E., Thordarson, T., Turnock, S., Barsotti, S., Delaney, L., Feng, W., Grainger, R.G., Hort, M.C., Höskuldsson, Á., Ialongo, I., Ilyinskaya, E., Jóhannsson, T., Kenny, P., Mather, T.A., Richards, N.A.D., Shepherd, J., 2015. Satellite detection, long-range transport, and air quality impacts of volcanic sulfur dioxide from the 2014–2015 flood lava eruption at Bárðarbunga (Iceland). Journal of Geophysical Research: a 120, 1–17. https://doi.org/10.1002/2014JC010485.Received

Sigurgeirsson, M.A., 2004. Þáttur úr gossögu Reykjaness. Náttúrufræðingurinn 72, 21–28.

Smythe, D.J., Wood, B.J., Kiseeva, E.S., 2017. The S content of silicate melts at sulfide saturation: New experiments and a model incorporating the effects of sulfide composition. American Mineralogist 102, 795–803. https://doi.org/10.2138/am-2017-5800CCBY

Stewart, C., Damby, D.E., Horwell, C.J., Elias, T., Ilyinskaya, E., Tomašek, I., Longo, B.M., Schmidt, A.,

Carlsen, H.K., Mason, E., Baxter, P.J., Cronin, S., Baxter, P.J., 2022. Volcanic air pollution and human health: recent advances and future directions. *Bulletin of Volcanology*, *84*(1), p.11.Thordarson, T., Self, S., Miller, D.J., Larsen, G. and Vilmundardóttir, E.G., 2003. Sulphur release from flood lava eruptions in the Veidivötn, Grímsvötn and Katla volcanic systems, Iceland. *Geological Society, London, Special Publications*, *213*(1), pp.103-121.

Weiser, F., Baumann, E., Jentsch, A., Medina, F.M., Lu, M., Nogales, M., Beierkuhnlein, C., 2022. Impact of Volcanic Sulfur Emissions on the Pine Forest of La Palma, Spain. Forests 13. https://doi.org/10.3390/f13020299

Wieser, P.E., Gleeson, M., 2022. PySulfSat: An Open-Source Python3 Tool for modelling sulfide and sulfate saturation.

Number	Eruptive unit	Acronym	Volcanic system	Age	$C_{S\ MI}$	C_{glass}	ΔC_S	V	V_{DRE}	Mass	M_S	Potential M_S	MOR[b]	Time of lava emplacement	Daily SO_2 emissions
				A.D.	ppm	ppm	ppm	km^3	km^3	Kg	Mt	Mt	m^3/s	days	tons/day
1	Stampahraun 4	SO	Reykjanes	1210-1240	1559	258	1275	0.10	0.09	2.3E+11	0.58	0.71	6.4 - 67.9 (17.9)	17 - 193 (65)	3570 - 40450 (10620)
2	Arnarseturshraun	SÖ-A	Svartsengi	1210-1240	1907	196	1667	0.55	0.47	1.3E+12	4.23	4.81	26.1 - 60.1 (33.5)	106 - 244 (190)	20420 - 47000 (26200)
3	Eldvarpahraun	SÖ-E	Svartsengi	1210-1240	1907	112	1759	0.28	0.24	6.4E+11	2.26	2.45	26 - 93.7 (33.3)	35 - 125 (97)	21340 - 76900 (27300)
4	Illahraun	SÖ-I	Svartsengi	1210-1240	1907	312	1563	0.05	0.04	1.1E+11	0.36	0.44	4 - 42.7 (11.2)	14 - 145 (52)	2920 - 31140 (8180)
5	Sundhnúkar Dec. 2023	Sund 2023	Svartsengi	2023	1610	210	1372	0.011[d]	0.01	2.5E+10	0.07	0.08	50[d]	2.5	32000
6	Sundhnúkar Jan. 2024*	Sund 2024a	Svartsengi	2024	1400	160	1215	-	-	-	-	-	-	<2	-
7	Sundhnúkar Feb. 2024*	Sund 2024b	Svartsengi	2024	1607	164	1414	-	-	-	-	-	-	<2	-
8	Fagradalsfjall 2021	Fagra 2021	Fagradalsfjall	2021	1170	20	1127	0.15[c]	0.13	4.1E+11	0.78	0.80	9.5[c]	185	5000
9	Fagradalsfjall 2022	Fagra 2022	Fagradalsfjall	2022	1300	120	1180	0.011[d]	0.01	2.5E+10	0.06	0.07	7.0[d]	18	3780
10	Fagradalsfjall 2023	Fagra 2023	Fagradalsfjall	2023	1170	120	1050	0.015[d]	0.013	3.4E+10	0.07	0.08	7.0[d]	26	3360
11	Ögmundarhraun	ÖGM	Krýsuvík	1151-1188	1517	138	1351	0.13	0.11	3.0E+11	0.81	0.90	31.9 - 73.3 (40.8)	21 - 47 (37)	20110 - 46220 (25750)
12	Kapelluhraun	KAP	Krýsuvík	1151-1188	1482	183	1273	0.07	0.06	1.6E+11	0.41	0.48	20.2 - 213 (56)	4 - 40 (14)	12000 - 126500 (33240)
13	Mávahlíðarhraun	MÁH	Krýsuvík	1151-1188	1297	280	997	0.02	0.02	4.6E+10	0.09	0.12	5.8 - 61 (16)	4 - 40 (14)	2700 - 28370 (7450)
14	Hrútafellshraun[a]	HRF	Krýsuvík	8^{th} - 9^{th} century	1546	252	1268	0.04[a]	0.03	9.0E+10	0.23	0.28	11.4 - 120 (31.5)	4 - 40 (14)	6750 - 71000 (18660)
15	Hvammahraun	h128	Brennisteinsfjöll	8^{th} - 9^{th} century	1900	90	1810	0.72	0.61	1.7E+12	5.86	6.27	48.3 - 510.6 (134.1)	16 - 173 (62)	39970 - 422560 (111000)
16	Kistuhraun	h130	Brennisteinsfjöll	900-1100	1494	94	1372	0.08	0.07	1.8E+11	0.50	0.55	6.1 - 22 (7.8)	42 - 152 (119)	3900 - 14000 (5000)
17	Selvogshraun	h138	Brennisteinsfjöll	10^{th} - 11^{th} century	1504	126	1350	0.19	0.16	4.4E+11	1.18	1.31	14.2 - 149.9 (39.4)	15- 155 (56)	8950 - 94450 (24810)
18	Tvíbollahraun	tv	Brennisteinsfjöll	950	1367	129	1213	0.37	0.31	8.5E+11	2.06	2.32	18.7 - 43 (24)	100 - 229 (178)	10580 - 24340 (13580)
19	Svartihryggur[a]	h142	Brennisteinsfjöll	900-1200	1341	147	1170	0.0005[a]	0.0004	1.3E+09	0.003	0.003	0.5 - 3.3 (2)	2 - 13 (3)	270 - 1800 (1100)
20	Húsfellsbruni[a]	Hú1 & Hú2	Brennisteinsfjöll	9 - 13^{th} century	1739	55	1650	0.20[a]	0.17	4.9E+11	1.62	1.70	50.6 - 116.4 (64.9)	21 - 49 (38)	38960 - 89620 (50000)
21	Kristnitökuhraun[a]	KRT	Brennisteinsfjöll	1000	1640	118	1492	0.06[a]	0.05	1.4E+11	0.41	0.45	14.1 - 50.9 (18)	14 - 50 (39)	9800 - 35420 (12570)

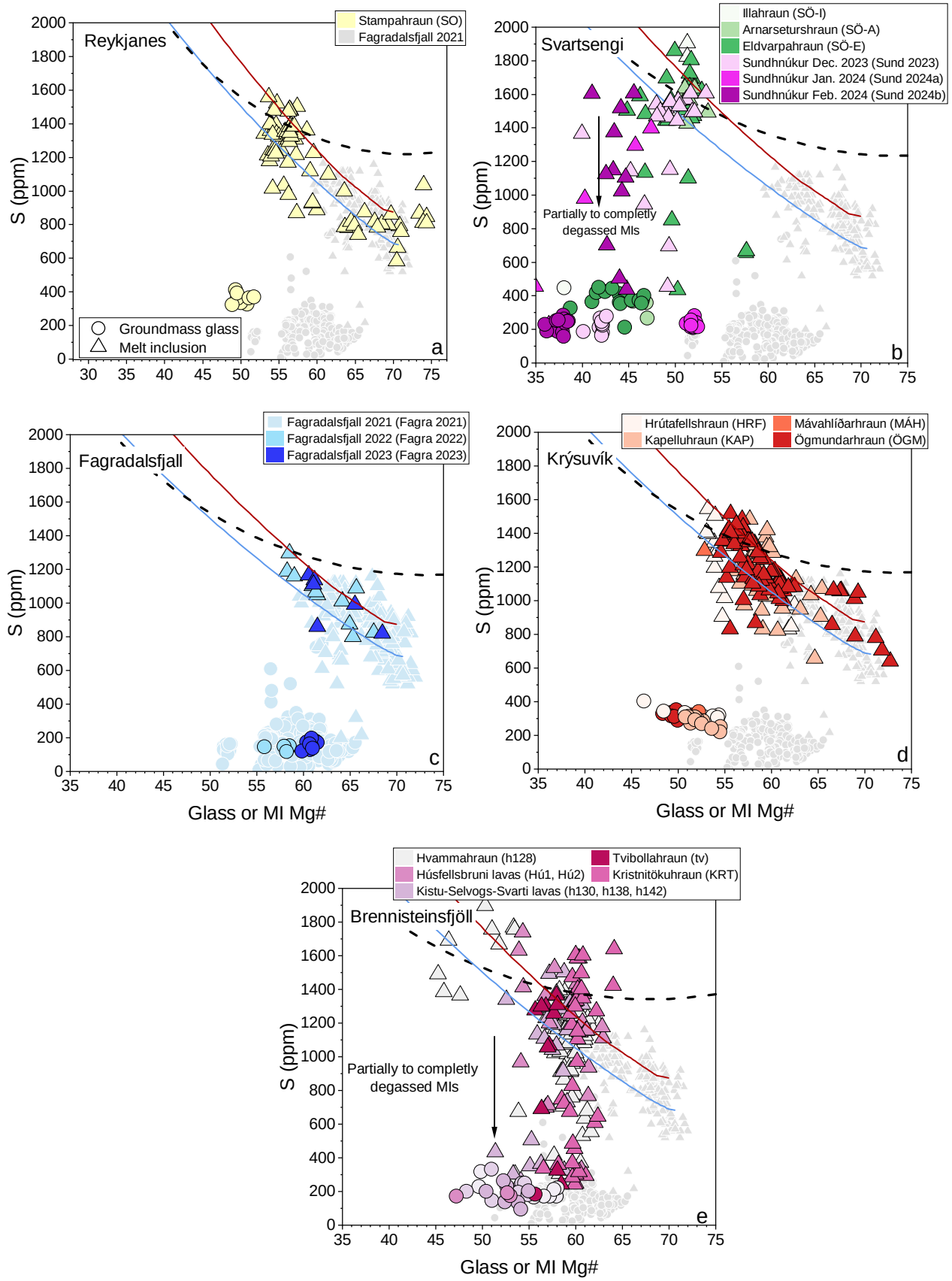
Reykjanes
Stampahraun (SO)
Fagradalsfjall 2021
Groundmass glass
Melt inclusion
a
Svartsengi
Illahraun (SÖ-I)
Arnarseturshraun (SÖ-A)
Eldvarpahraun (SÖ-E)
Sundhnúkur Dec. 2023 (Sund 2023)
Sundhnúkur Jan. 2024 (Sund 2024a)
Sundhnúkur Feb. 2024 (Sund 2024b)
Partially to completly degassed MIs
b
Fagradalsfjall
Fagradalsfjall 2021 (Fagra 2021)
Fagradalsfjall 2022 (Fagra 2022)
Fagradalsfjall 2023 (Fagra 2023)
c
Krýsuvík
Hrútafellshraun (HRF)
Kapelluhraun (KAP)
Mávahlíðarhraun (MÁH)
Ögmundarhraun (ÖGM)
d
Brennisteinsfjöll
Hvammahraun (h128)
Húsfellsbruni lavas (Hú1, Hú2)
Kistu-Selvogs-Svarti lavas (h130, h138, h142)
Tvibollahraun (tv)
Kristnitökuhraun (KRT)
Partially to completly degassed MIs
e
S (ppm)
Glass or MI Mg#

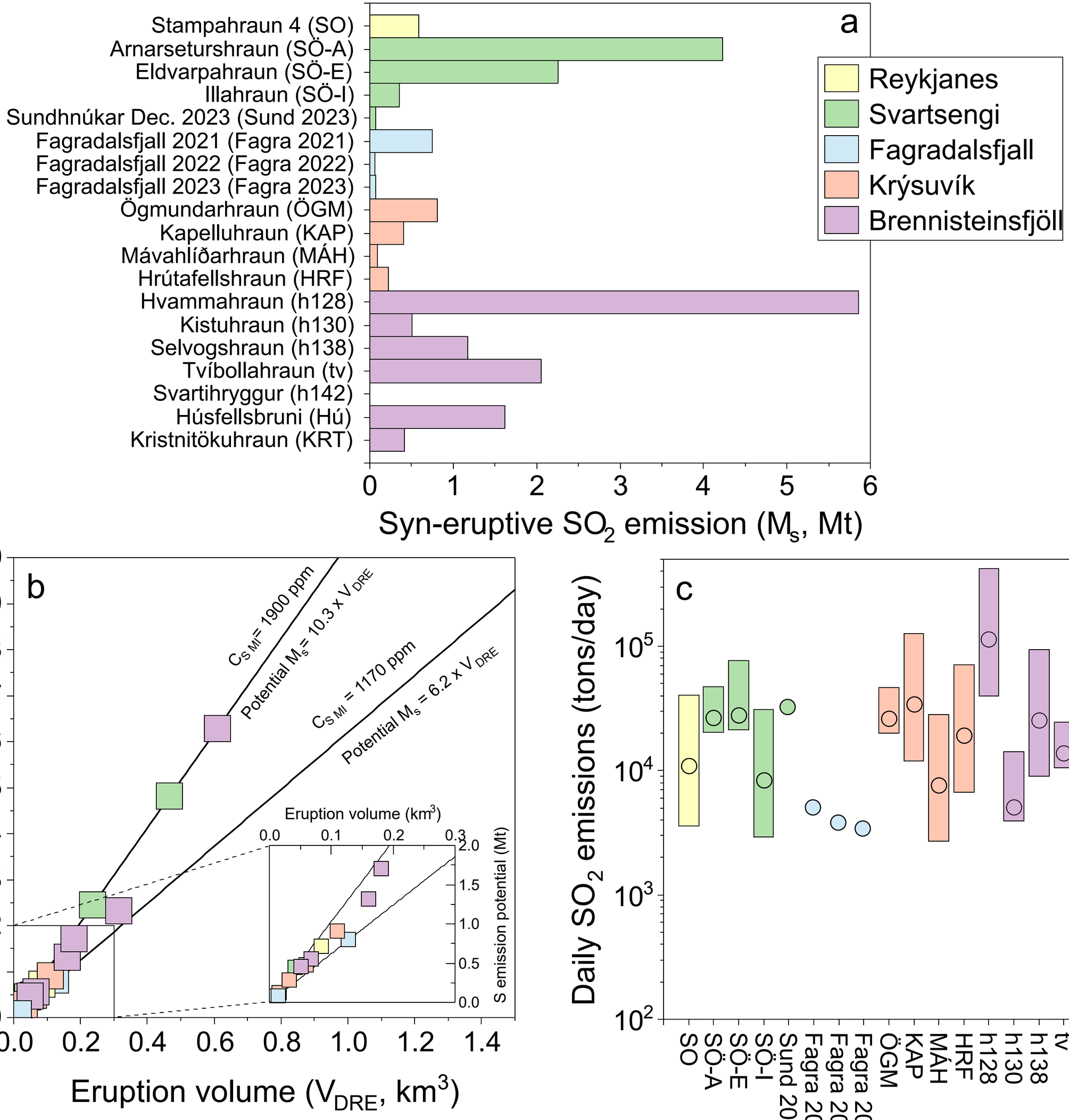
a
Stampahraun 4 (SO)
Arnarseturshraun (SÖ-A)
Eldvarpahraun (SÖ-E)
Illahraun (SÖ-I)
Sundhnúkar Dec. 2023 (Sund 2023)
Fagradalsfjall 2021 (Fagra 2021)
Fagradalsfjall 2022 (Fagra 2022)
Fagradalsfjall 2023 (Fagra 2023)
Ögmundarhraun (ÖGM)
Kapelluhraun (KAP)
Mávahlíðarhraun (MÁH)
Hrútafellshraun (HRF)
Hvammahraun (h128)
Kistuhraun (h130)
Selvogshraun (h138)
Tvíbollahraun (tv)
Svartihryggur (h142)
Húsfellsbruni (Hú)
Kristnitökuhraun (KRT)
Reykjanes
Svartsengi
Fagradalsfjall
Krýsuvík
Brennisteinsfjöll
0
1
2
3
4
5
6
Syn-eruptive SO2 emission (Ms, Mt)
b
Potential SO2 emission (Mt)
CS MI= 1900 ppm
Potential Ms= 10.3 x V DRE
CS MI = 1170 ppm
Potential Ms = 6.2 x V DRE
Eruption volume (km3)
S emission potential (Mt)
Eruption volume (VDRE, km3)
c
Daily SO2 emissions (tons/day)
2021 Fagradalsfjall SO2 emissions
SO
SÖ-A
SÖ-E
SÖ-I
Sund 2023
Fagra 2021
Fagra 2022
Fagra 2023
ÖGM
KAP
MÁH
HRF
h128
h130
h138
tv
h142
Hú
KRT

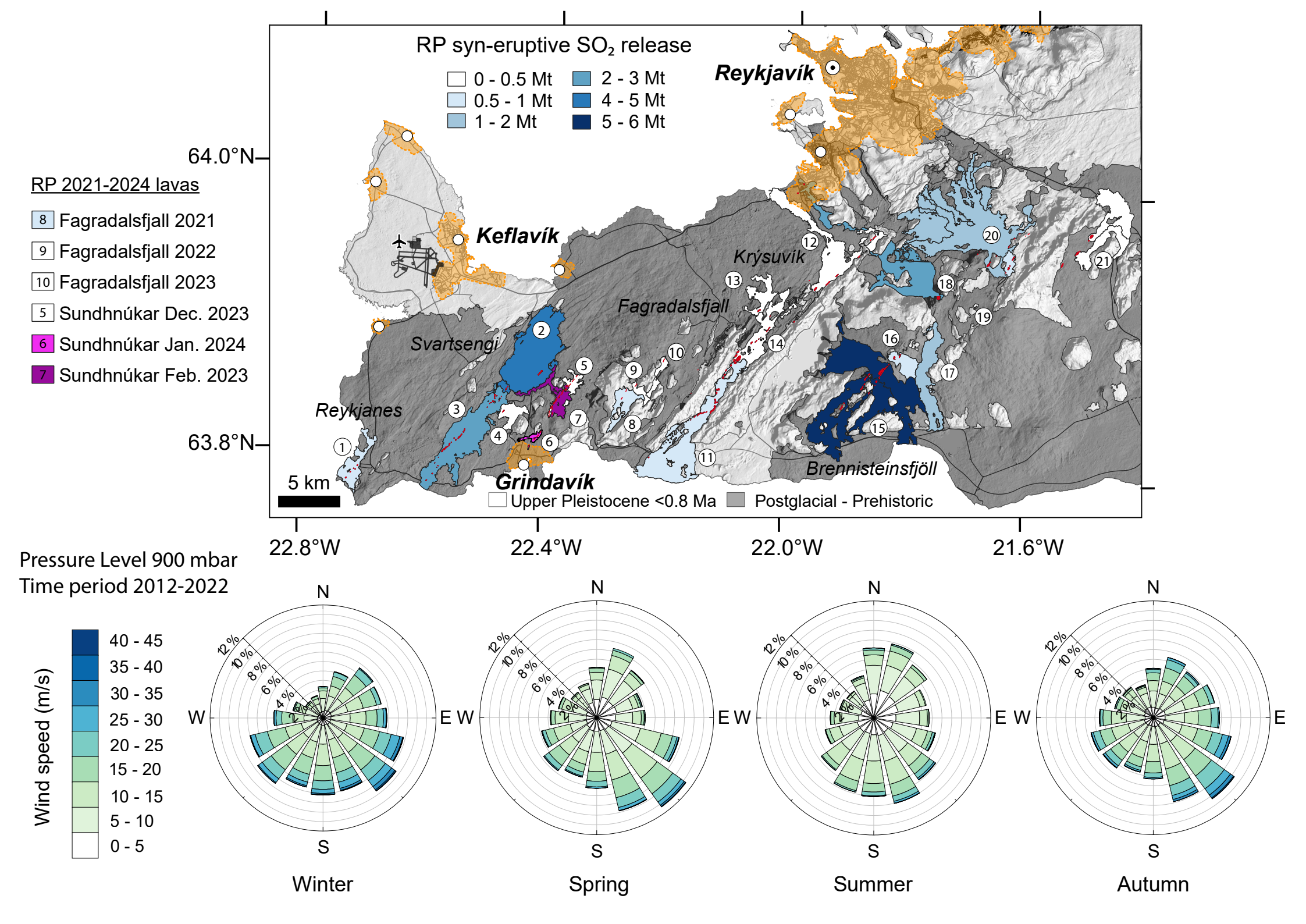
RP syn-eruptive SO2 release
0 - 0.5 Mt
0.5 - 1 Mt
1 - 2 Mt
2 - 3 Mt
4 - 5 Mt
5 - 6 Mt
RP 2021-2024 lavas
8 Fagradalsfjall 2021
9 Fagradalsfjall 2022
10 Fagradalsfjall 2023
5 Sundhnúkar Dec. 2023
6 Sundhnúkar Jan. 2024
7 Sundhnúkar Feb. 2023
Reykjavík
Keflavík
Krýsuvík
Fagradalsfjall
Svartsengi
Reykjanes
Grindavík
Brennisteinsfjöll
5 km
Upper Pleistocene <0.8 Ma
Postglacial - Prehistoric
64.0°N
63.8°N
22.8°W
22.4°W
22.0°W
21.6°W
Pressure Level 900 mbar
Time period 2012-2022
Wind speed (m/s)
40 - 45
35 - 40
30 - 35
25 - 30
20 - 25
15 - 20
10 - 15
5 - 10
0 - 5
N
S
W
E
12 %
10 %
8 %
6 %
4 %
2 %
Winter
Spring
Summer
Autumn